Machine-Learning-Based Accurate Finger Joint Stiffness Estimation With Joint Modular Soft Actuators

Fuko Matsunaga, Ema Oba, Ming-Ta Ke, Ya-Hsin Hsueh, Shao Ying Huang, Jose Gomez-Tames, and Wenwei Yu, *Member, IEEE*

***Abstract*—Finger joint stiffness assessment is very important in quantifying the degree of disability in stroke patients and determining rehabilitation strategies and plans. However, the evaluation methods used in clinical practice rely heavily on the experience of clinicians. In our previous study, we adapted an analytical model originally proposed for a whole-finger soft actuator to objectively quantify joint stiffness by using a new type of joint modular soft actuator designed for individualized hand rehabilitation. However, stiffness could not be accurately estimated owing to the effects of the interaction between joint modular soft actuators and a finger, as well as, between the actuators themselves, which could not be represented by the adapted analytical model. In this study, artificial neural network (ANN)-based models were proposed to simultaneously quantify the stiffness of three joints using joint modular soft actuators and compared with the adapted analytical model and other machine-learning (ML)-based models. Moreover, the estimation performance was verified for high stiffness values and different finger sizes. The results show that the ANN-based models estimate stiffness more stably and accurately than the adapted analytical and other ML-based models. This study shows the feasibility of quantitative evaluation of joint stiffness using joint modular soft actuators.**

***Index Terms*—Deep learning methods, rehabilitation robotics, soft robot applications.**

I. Introduction

FINGER flexor spasticity is a common aftereffect of stroke [1]. It not only increases the stiffness of the fingers but also decreases the range of motion, thereby affecting the recovery of a patient's motor function [2]. Therefore, understanding a patient's spasticity condition may help therapists to determine the optimal rehabilitation [3]. The assessment of the spasticity condition regularly adopted in rehabilitation is based on clinical scales, such as the Modified Ashworth Scale (MAS) [4]. However, the lack of objectivity in such evaluation methods is a problem because these methods rely heavily on the experience of clinicians [5], [6].

The assessment of finger joint stiffness is very important for quantifying the impairment of stroke patients and determining rehabilitation strategies and plans [7]. The dedicated stiffness measurement devices developed to date are large and heavy because they consist of many rigid parts, and it is also difficult to evaluate each finger joint separately [8], [9], [10]. Heung et al. developed a system that combines finger motion support and finger stiffness evaluation functions by estimating the stiffness of finger joints using an analytical model of a soft elastic composite actuator (SECA) [11]. Using the SECA facilitated the incorporation of a function for estimating the stiffness of individual joints into rehabilitation training, thus suggesting the possibility of providing patients with optimal training exercises and assistance with activities of daily living.

However, whole-finger soft actuators such as the SECA, which have a structure with multiple air chambers connected, have only one air pressure input and cannot assist joints individually. Therefore, providing detailed joint-level motion support for hand rehabilitation is difficult. Furthermore, whole-finger soft actuators require changes in actuator dimensions to accommodate individual differences, such as finger size; therefore, designing and prototyping individual customizations require a considerable time, making timely rehabilitation difficult. To address this problem, joint modular soft actuators that consist of multiple sections corresponding to each finger joint have been developed [12], [13], [14]. Joint modular soft actuators provide high bending performance with minimal energy and can accommodate individual differences with minimal effort.

In our previous work [15], we adapted the analytical model originally proposed for the SECA to objectively quantify joint stiffness by using a new modular version of the SECA (Modular-SECA), which allowed us to deal with individual joints for rehabilitation and stiffness evaluation. Correction parameters were added to the SECA's analytical model to estimate the stiffness of

Manuscript received 7 May 2024; accepted 4 June 2024. Date of publication 18 June 2024; date of current version 28 June 2024. This letter was recommended for publication by Associate Editor V. Ruiz Garate and Editor P. Valdastri upon evaluation of the reviewers' comments. This work was supported by the Grant-in-Aid for Scientific Research (B), JSPS KAKENHI under Grant 22H03450. *(Corresponding author: Wenwei Yu.)*

Fuko Matsunaga and Ema Oba are with the Graduate School of Engineering, Chiba University, Chiba 2638522, Japan (e-mail: matsunagafuko@chiba-u.jp; 24wm4211@student.gs.chiba-u.jp).

Ming-Ta Ke is with the Graduate School of Intelligent Data Science, National Yunlin University of Science and Technology, Yunlin 64002, Taiwan (e-mail: kemingta@yuntech.edu.tw).

Ya-Hsin Hsueh is with the Department of Electronic Engineering, National Yunlin University of Science and Technology, Yunlin 64002, Taiwan (e-mail: hsuehyh@yuntech.edu.tw).

Shao Ying Huang is with the Engineering Product Development pillar, Singapore University of Technology and Design, Singapore 487372 (e-mail: huangshaoying@sutd.edu.sg).

Jose Gomez-Tames and Wenwei Yu are with the Graduate School of Engineering, Chiba University, Chiba 2638522, Japan, and also with the Center for Frontier Medical Engineering, Chiba University, Chiba 2638522, Japan (e-mail: jgomez@chiba-u.jp; yuwill@faculty.chiba-u.jp).

Digital Object Identifier 10.1109/LRA.2024.3416073

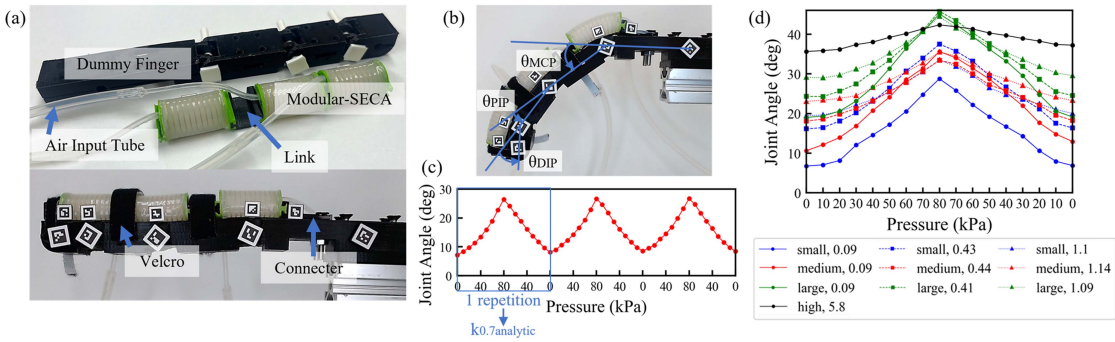

Fig. 1. (a) Modular-SECA, dummy finger design and modular-SECA attached to dummy finger, (b) joint angles, (c) three repetitions contained in one measurement in the stiffness estimation experiment; one $k_{0.7analytic}$ is calculated from each repetition, (d) the pressure-angular change profiles for 10 of the 180 samples for the MCP joint of three sizes of dummy fingers (small, medium, and large). The label high is the pressure-angular change profile with a high stiffness torsion spring attached to the medium-sized dummy finger. The numbers in the legend denote the value of their k_{spring}.

the metacarpophalangeal (MCP) joint with the Modular-SECA. The analytical model adapted to the Modular-SECA is denoted as the adapted analytical model.

However, the accuracy of joint stiffness estimation was insufficient because the adapted analytical model could not represent the characteristics of the Modular-SECA. The Modular-SECA had rigid connectors attached at both ends. Thus, the bending performance of the actuator as well as the interaction between the finger and the actuator when the actuator was worn on the finger were different from those of the SECA. Moreover, the influence of the interaction differed depending on how the Modular-SECA was attached to the finger, which could not be represented by the adapted analytical model. In addition, the Modular-SECA supported the distal interphalangeal (DIP), proximal interphalangeal (PIP), and MCP joints individually, and the three Modular-SECAs were connected using connectors. Therefore, the same adapted analytical model could not be applied to all joints because the bending behavior of the Modular-SECA was different for each joint owing to the effects of the interaction between the Modular-SECAs themselves. These factors make improving the accuracy of joint stiffness estimation with the Modular-SECAs using the adapted analytical model difficult.

In this study, we aimed to simultaneously estimate the stiffness of three finger joints with the Modular-SECAs. Four different artificial neural network (ANN)-based models were proposed and compared with the adapted analytical model. We expected that the ANN models could deal with the effects of interaction and super-elasticity, such as strong nonlinearity and inconsistency in the bending behavior of different joints, caused by using joint modular soft actuators for rehabilitation and joint stiffness estimation. In addition, ANN-based models were also compared with other machine-learning (ML) algorithm-based models to verify that ANN is the best ML algorithm for stiffness estimation. The best model was determined by comparing the stiffness estimation results. The feasibility of estimating joint stiffness for high stiffness values (which could not be estimated previously) and fingers of different sizes was also verified.

II. Method

This section first explains the adapted analytical model and stiffness measurement experiments. After this, the ANN-based models, the other ML-based models, and the selection criteria for the best model are explained.

A. Design of Modular-SECA and Dummy Finger

The soft actuators used in this study were the Modular-SECAs based on our previous study (Fig. 1(a)) [15]. Dummy fingers imitating three different sizes of Japanese index fingers (small, medium, and large) were designed based on [13]. Torsion springs with different spring constants were placed at the dummy finger joints (DIP, PIP, and MCP) to vary the finger joint stiffness.

B. Estimation of Joint Stiffness by Prototype Experiment

The adapted analytical model for finger joint stiffness estimation using the Modular-SECA is shown in (1) [15].

$$k_{0.7} = \frac{2\left(W_A + 0.5\,W_L - 1.15\,W_P\right)}{\left(\theta - \theta_0\right)^2}, \theta \in [0, 0.7\theta_0)\,, \quad (1)$$

where W_A, W_L, and W_P are the bending strain energy stored in the silicone body of the Modular-SECA, the bending strain energy stored in the torque compensation layer, and the work done by the input air pressure, respectively. Furthermore, $k_{0.7}$, θ, and θ_0 are joint stiffness, joint angle, and resting angle, respectively.

In [15], estimations were made for just two stiffness levels (low and medium). However, the accuracy of these estimations alone may not suffice for actual evaluations. This limitation becomes evident when comparing finger stiffness values pre and post rehabilitation such as in [16]. Specifically, when the variation in stiffness measurements is small (e.g., 0.1 Nmm/deg [16]), evaluating the effects of rehabilitation becomes challenging with only ordinal estimations.

Therefore, in this study, to perform multiple-level or even continuous estimation, nine joint stiffness values near the low and medium stiffness levels defined based on stiffness values of MAS $\leq 1+$ were set as the target values for the prototype experiment and learning and validation of the estimation models [15]. Torsion springs with spring constants corresponding to the nine joint stiffness values, denoted as k_{spring} (as shown in Table I) were placed at each of the three joints (DIP, PIP, and MCP). The joint stiffness value was set not as the nominal

TABLE I
TARGET STIFFNESS VALUES OF THE MEDIUM-SIZED DUMMY FINGER IN THE STIFFNESS ESTIMATION EXPERIMENT

Joint	Target Joint Stiffness Values (Nmm/deg)								
	Level 1	*Level 2*	*Level 3*	*Level 4*	*Level 5*	*Level 6*	*Level 7*	*Level 8*	*Level 9*
DIP	0.10	0.25	0.41	0.53	0.90	1.07	1.35	2.60	2.67
PIP	0.09	0.22	0.39	0.47	0.79	0.97	1.17	2.03	2.46
MCP	0.09	0.22	0.35	0.44	0.74	0.92	1.14	1.96	2.32

spring constant of the torsion spring but measured by applying a weight onto the dummy phalange of the dummy finger with the torsion spring placed in its joint. This is because, in the current experiment setting, the effective spring constant may differ from the nominal value. When using a torsion spring, a shaft with a suitable size is important because the inner diameter of the torsion spring changes as it deforms under a loading, whereas setting optimal shafts for various torsion springs at different joints is difficult.

In the prototype experiment, the Modular-SECAs attached to the DIP, PIP, and MCP joints of the dummy finger were simultaneously pressurized from 0 kPa to a maximum air pressure of 80 kPa and then depressurized again to 0 kPa to complete one repetition. The bending performance of the Modular-SECA's $0-80$ kPa is equal to or even better than that of the SECA's $0-160$ kPa [11], [15]. Therefore, a pressure setting of $0-80$ kPa is sufficient for both estimating joint stiffness and supporting finger motions using the Modular-SECAs. Moreover, the smaller maximum air pressure was used for even a lower safety risk. The relationship between the air pressure values in one repetition and the resultant joint angles of the dummy finger is denoted as the pressure-angular change profile. The joint angles of the DIP, PIP, and MCP were measured at every 10 kPa (Fig. 1(b)). In [17], the repetition number in each measurement was set to three for human subjects to prevent the short-term effects of any stretch, for example, loosening and/or reduction of the muscle tone of the joints, from affecting the stiffness estimation results. Therefore, in this study, the same repetition number (three), was considered as one measurement (Fig. 1(c)), and the repeatability was also verified by performing three measurements at each stiffness level. Before each measurement, the resting angles of the dummy finger were measured, and the Modular-SECAs were attached to the dummy finger to initiate the measurement. After the measurements, the stiffness values of the joints at each pressure were obtained in the range of $\theta\in[0, 0.7\theta_0)$ using (1). Finally, the stiffness values, $k_{0.7}$, obtained in one repetition, were averaged using (2) to determine the final joint stiffness, $k_{0.7analytic}$.

$$k_{0.7amalytic} = \frac{1}{n}\sum_{i=1}^{n} k_{0.7i}, (1 \le n \le 17) \tag{2}$$

where n is the number of joint angles that are included in the stiffness estimation range among the 17 joint angle values measured from one repetition. This is the stiffness estimation method using the adapted analytical model.

TABLE II
ANN-BASED STIFFNESS ESTIMATION MODELS PROPOSED

Network	*Input*	*Output*
MLP	θ×17	k_{spring}
		Δk
CNN		k_{spring}
		Δk

C. ANN-Based Stiffness Estimation Model

The four ANN-based stiffness estimation models proposed are listed in Table II.

Instead of calculating one stiffness value for each pressure-angular change profile and then averaging all the values for different angular points to obtain an estimated stiffness, this ANN approach fully utilizes the total pressure-angular change profile of each measurement. Hence, 17 joint angle values from one repetition (Fig. 1(c)) were used as input to each ANN model. Two types of output variables were considered for the model: one is the stiffness value of each finger joint, with the target value of k_{spring}; the other is Δk denoted in (3), which is the difference between the stiffness value estimated using the adapted analytical model and k_{spring}.

$$\Delta k = k_{lanalytic} - k_{spring}. \tag{3}$$

As the ANN models for predicting Δk use the adapted analytical model, we expected that information contained in the adapted analytical model may help guide the learning. In this case, the stiffness value estimated using the adapted analytical model was not $k_{0.7analytic}$ but $k_{1analytic}$, which was obtained by changing the stiffness estimation range in (1) to that in (4) and averaging the resultant stiffness, k_1, using (5).

$$k_1 = \begin{cases} \frac{2(W_A+0.5W_L-1.15W_P)}{(\theta-\theta_0)^2}, \theta \in [0, 0.7\theta_0) \\ \frac{2(W_A+0.5W_L-1.15W_P)}{(0.7\theta_0-\theta_0)^2}, \theta \in [0.7\theta_0, \theta_0) \end{cases} \tag{4}$$

$$k_{lanalytic} = \frac{1}{n}\sum_{i=1}^{n} k_{1i}, (1 \le n \le 17). \tag{5}$$

In the adapted analytical model, the range was limited by adding an empirical coefficient of 0.7 to the estimation range, as in $\theta\in[0, 0.7\theta_0)$, to stabilize the accuracy without giving the effect of the singularity where the denominator of (1) becomes close to zero near $\theta = \theta_0$ to the analytical model; thus, some measurements could not be used to estimate joint stiffness. Since we expected that the ANN may learn to some extent without the effect of the values near the singularity, extending the stiffness estimation range to $\theta\in[0, \theta_0)$ is possible. However, in the ANNs for predicting Δk, if the stiffness values are estimated using (1) even after the joint angle exceeds $0.7\theta_0$, the Δk becomes very

large, and the prediction accuracy of the ANN may be low. This is because if the measured θ value was even slightly larger than the theoretical θ value (small angle error) in $\theta \in [0.7\theta_0, \theta_0)$, the $k_{0.7}$ estimated from (1) becomes very large, and the error (i.e., Δk) between $k_{0.7analytic}$ and k_{spring} becomes very large. Thus, to stabilize the accuracy of the ANN for $\theta \in [0.7\theta_0, \theta_0)$, for the ANN models predicting Δk, we reset the value to $0.3\theta_0$ if $(\theta - \theta_0)$ in the denominator of the adapted analytical model was smaller than $0.3\theta_0$, as shown in (4). The coefficient of 0.3 for the reset value was chosen based on the stability of the prediction accuracy and the amount of change in the denominator value due to the reset.

The effectiveness of using ML to accurately predict the complex behavior of soft actuators has been shown [18]. Therefore, the use of ML is also expected to be effective in stiffness estimation with the Modular-SECA. Among ML algorithms, ANN tends to have superior generalization capabilities than other ML algorithms because it automatically learns effective features hidden deep in data instead of relying on manually designed features [19]. This characteristic makes ANN widely used for learning complex and nonlinear relationships [20]. Hence, we considered it a suitable algorithm for the stiffness estimation task in this study, which involves various interactions and nonlinear influencing factors such as finger size and variability due to attachment during measurements. The ANNs used included a multilayer perceptron (MLP) and a convolutional neural network (CNN), considering the training data set's size and characteristics. MLP is the most canonical type of ANN. CNN has been widely used for tasks involving image processing and time series analysis because it can extract deeper features from input data, making it robust against noise [19], [21]. Therefore, a CNN was expected to extract useful features from the pressure-angular change profiles (Fig. 1(c)), leading to a model with excellent generality. Thus, we compared the CNN with the MLP, which is a simple structured feed-forward neural network with only multiple linear layers, to verify whether the characteristics of the CNN are adequate for our dataset.

The MLP contains two hidden layers, each with 17 neurons. Immediately following each hidden layer are an activation function and a dropout layer (dropout rate: 0.1), i.e., the MLP has two dropout layers. The CNN contains two convolutional layers and two linear layers with 17 nodes. The output channels in the first and second convolutional layers are 68 and 128, respectively. The CNN utilizes the kernel size of two and boundary padding of one in the convolutional layers. Immediately following the convolutional layers and the first linear layer are an activation function and a dropout layer (dropout rate: 0.1), i.e., the CNN has three dropout layers. The activation function for both models is ReLu. Adam is used as the optimization function, and each neural network was trained 500 epochs with a learning rate of 1e-4 and weight decay of 1e-4. These parameters were determined by using 8-fold cross-validation to balance overfitting and underfitting. All models were developed with Python 3.9.12 64-bits. PyTorch 2.1.2+cu118 was used to build the neural networks.

The data from the prototype experiment with the medium-sized dummy finger were used to train and test the ANN models. The test data were set up to include one sample for each stiffness level. Input data were standardized as a pre-processing step before being inputted into the models. The same type of ANN was built for each joint, creating three ANNs for one finger. All experimental data used to train and test the models was made available online at [22]. The prediction using data from the medium-sized dummy finger is denoted as M-Test.

Furthermore, the generality of the ANN models was verified by using two additional stiffness predictions. First, because the analytical model of (1) used in [15] had a small estimation range, some k_{spring} could not be estimated. However, the ANN models may be able to estimate stiffness values that were impossible to estimate previously. Therefore, the prediction performance for high stiffness was verified by measuring the angles of the medium-sized dummy finger at the k_{spring} values (DIP: 5.71, PIP: 5.45, and MCP: 5.80), which were considerably larger than those used for training. These values were determined based on joint stiffness values with MAS $\geq$ 2 [8], [17]. Next, practical applications are only possible if the ANN model can be applied to estimate the stiffness of different finger sizes. Therefore, the prediction performance for different finger sizes was verified using the data obtained from the prototype experiments with the small and large-sized dummy fingers. The prediction for high stiffness values is denoted as H-Prediction, and the predictions using data from the small and large-sized dummy fingers are denoted as S-Prediction and L-Prediction, respectively. The H-Prediction, the S-Prediction, and the L-Prediction are collectively denoted as the generality test.

Fig. 1(d) shows the pressure-angular change profiles for 10 of the 180 samples of the M-Test and the generality test for the MCP joint. Even for equivalent values of k_{spring}, the angle trajectory differs depending on the finger size. Moreover, the magnitude of the angular change does not monotonically increase with k_{spring}, indicating a complex behavior. We expected that the ANN models that fully utilized the pressure-angular change profiles could be used to accurately estimate joint stiffness.

D. Other ML-Based Model

We selected a linear regression and a support vector machine as the ML algorithms to compare with the ANNs. A brief description of each algorithm is given below. More detailed information about them can be found in [23].

Linear Regression (LR): LR is a regression algorithm that models the relationship between an output variable and one or more input variables by fitting the relationship between the input and output data to a straight line or a hyperplane. LR aims to minimize the squared error between observed and predicted values and is unsuitable for learning nonlinear relationships. Thus, it was selected for a comparison to verify that the factors, which the adapted analytical model cannot represent, are nonlinear and that linear models are unsuitable for stiffness estimation models.

Support Vector Machine for Regression (SVR): Support Vector Machine (SVM) is an ML algorithm that can be used for classification and regression tasks. SVR is an extension of SVM made for continuous values. SVR aims to minimize the effect of outliers on the regression equations by taking the approach that

data points with residuals within the threshold do not contribute to the regression fit while data points with an absolute difference greater than the threshold contribute a linear-scale amount. It can handle both linear and nonlinear relationships using different kernel functions. While the ANNs can extract valuable features hidden in the input data, algorithms like SVM learn the input data directly as features. Therefore, to verify the effectiveness of ANN's feature extraction for stiffness estimation, the SVM, which is most commonly used in human movement biomechanics studies similar to the task of this study [20], was selected as a comparison algorithm.

The inputs and outputs of the LR and the SVR were the same as for the ANNs, and two models with different outputs were built for each joint. These models were developed with Python 3.9.12 64-bits using scikit-learn 1.3.2 python library LinearRegression and SVR. The parameters of the SVR were tuned using 8-fold cross-validation to balance overfitting and underfitting. As a result of the tuning, the regularization parameter (C = 16) that controls the trade-off between training error and model complexity, the parameter ($\varepsilon = 0.0625$) that defines the error tolerance, and a Gaussian radial basis function kernel with a shape parameter $\gamma = 0.125$ was used.

E. Selection of Best Stiffness Estimation Model

The ideal stiffness estimation model should offer consistent and accurate predictions despite changing measuring conditions and minimize estimation variability caused by complex influencing factors across measurements. Therefore, we determined the best model using two indices: the root mean squared percentage error (RMSPE) and mean absolute percentage deviation (MAPD) [24].

The RMSPE is the relative error calculated by (6). Since the predicted value scale differs for the H-Prediction from other datasets, the percentage error was used to compare with other datasets. The MAPD extends the mean absolute deviation to a relative deviation and is calculated by (7), which shows the relative variation of predictions at the same target stiffness value. The RMSPE was calculated for each joint in the M-Test and the generality test datasets. The MAPD was calculated for each joint in the generality test datasets because the M-Test has only one prediction for one target value. Then, the mean and mean absolute deviation (mad) of the four RMSPEs and three MAPDs obtained for each prediction dataset were calculated for each joint (denoted as the $\text{RMSPE}_{\text{all}}$, MAPD_{all}). A model with small values of the $\text{RMSPE}_{\text{all}}$ and MAPD_{all} can make excellent and stable predictions across various datasets and consistently have excellent result repeatability. Therefore, the best model was determined based on the $\text{RMSPE}_{\text{all}}$ and MAPD_{all} calculated from each prediction dataset.

$$\text{RMSPE} = \sqrt{\frac{1}{N}\sum_{i=1}^{N}\left(\frac{y_i - t_i}{t_i}\right)^2}\,100 \tag{6}$$

$$\text{MAPD} = \frac{100}{N}\sum_{i=1}^{N}\left|\frac{y_i - y_{mean\_i}}{y_{mean\_i}}\right| \tag{7}$$

where N, y_i, and t_i are the number of data, the predicted value, and the target stiffness value. Note that y_{mean_i} is not the mean of all predictions, but the mean of predictions at the same target stiffness value.

III. Results

A. Finger Joint Stiffness Estimation

Table III presents the RMSPE and MAPD of the stiffness estimates. The stiffness estimation results for the M-Test obtained using the adapted analytical model and the ANN models are shown in Fig. 2. The $k_{0.7analytic}$ is lower than the target stiffness value, k_{spring}, for most estimates (Fig. 2). Moreover, $k_{0.7analytic}$ does not monotonically increase with k_{spring}. The ML-based models other than the LR provide better estimation results than $k_{0.7analytic}$ (M-Test in Table III). The best model varies for each joint, but the CNN and the SVR exhibit better prediction accuracy than the MLP and the LR.

B. Predictive Performance for High Stiffness Values

Table IV shows the estimated stiffness values in the H-Prediction. The ML-based models can estimate stiffness values that cannot be estimated by (2). However, many models have differences between the prediction results and the target stiffness values can be observed. Also, unlike in the M-Test, the MLP and the LR often have better accuracy than the CNN and the SVR.

C. Predictive Performance for Different Finger Sizes

The stiffness estimates for the small and large-sized dummy fingers obtained using the adapted analytical model and the ANN models are shown in Fig. 3. Although the predictions of the ANN models do not monotonically increase with the target stiffness in some areas, many predictions have better accuracy than $k_{0.7analytic}$ (Table III). Only the MLP and the CNN for predicting k_{spring} have better the RMSPE and MAPD than $k_{0.7analytic}$ for all joints in the S-Prediction and the L-Prediction. The LR and the SVR have some predictions that are considerably less accurate than the ANNs.

D. Selection of Best Model

Table V presents the $\text{RMSPE}_{\text{all}}$ and MAPD_{all} for the prediction datasets. The ML-based models' values within Table V are illustrated in Fig. 4. The ML-based models have better the $\text{RMSPE}_{\text{all}}$ and MAPD_{all} than $k_{0.7analytic}$ in most cases. It can be observed that the CNN for predicting k_{spring} for the DIP, the CNN for predicting k_{spring} for the PIP, and the MLP for predicting k_{spring} for the MCP demonstrate better the $\text{RMSPE}_{\text{all}}$ and MAPD_{all} compared to other models (Fig. 4).

IV. Discussion

In [15], the estimated stiffness value, $k_{0.7analytic}$, of the MCP joint was larger than the target stiffness value, k_{spring}. However, for most cases in this study, $k_{0.7analytic}$ was estimated to be smaller than k_{spring}. This difference may be due to changes in the interaction between the Modular-SECAs

TABLE III
PREDICTION ACCURACY OF JOINT STIFFNESS ESTIMATION

Model		RMSPE (%)			RMSPE (%) / MAPD (%)								
		M-Test			*H-Prediction*			*S-Prediction*			*L-Prediction*		
		DIP	***PIP***	***MCP***	***DIP***	***PIP***	***MCP***	***DIP***	***PIP***	***MCP***	***DIP***	***PIP***	***MCP***
$k_{0.7analytic}$		181	228	57				149 / 193	312 / 17	77 / 34	274 / 34	487 / 74	139 / 20
MLP	k_{spring}	21	88	37	31 / 5	**26** / 2	41 / 2	87 / **9**	25 / 7	43 / 14	37 / **12**	73 / 11	**90** / 8
	Δk	62	55	17	37 / 10	38 / 4	49 / 4	133 / 12	81 / 14	79 / 23	111 / 60	216 / 19	101 / 23
CNN	k_{spring}	**12**	36	10	42 / **3**	35 / 2	59 / 1	**70** / 16	**21** / **5**	54 / **13**	**36** / **12**	**39** / **9**	131 / 10
	Δk	14	**23**	**9**	64 / 4	36 / 5	**31** / 4	77 / 15	100 / 11	66 / 33	124 / 30	261 / 23	278 / 82
LR	k_{spring}	107	57	89	37 / **3**	32 / 2	48 / 3	121 / 49	225 / 81	562 / 34	153 / 68	135 / 22	151 / 14
	Δk	399	49	165	**15** / 12	55 / 5	59 / 4	179 / 246	265 / 87	232 / 21	243 / 75	258 / 181	148 / 45
SVR	k_{spring}	36	35	22	76 / 24	76 / **0**	84 / **0**	102 / 15	51 / 11	243 / **13**	70 / 20	69 / 13	300 / **5**
	Δk	60	25	20	26 / 24	49 / 4	71 / 4	75 / 16	69 / 152	**39** / **13**	194 / 32	274 / 20	178 / 19

Bold numbers indicate the ML-based model with the best prediction accuracy.

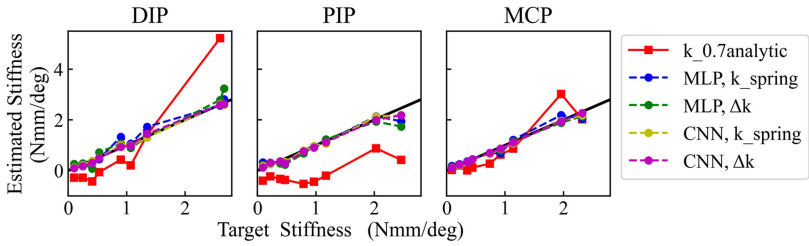

Fig. 2. Results of stiffness estimation on the medium-sized dummy finger. Stiffness values were estimated using the adapted analytical model and the ANN models for each of the nine target stiffness values. The black diagonal line indicate that the target stiffness value and the stiffness estimate coincide.

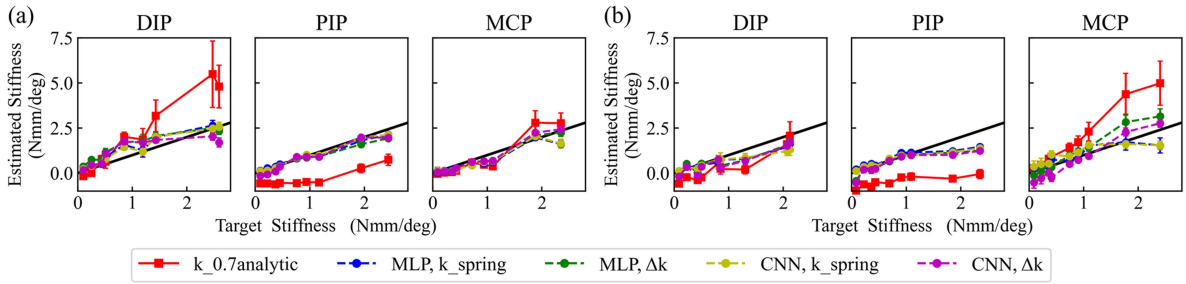

Fig. 3. Results of joint stiffness estimation on different size dummy fingers. Stiffness values were estimated using the adapted analytical model and the ANN models for each of the nine target stiffness values (mean and standard deviation of nine estimated stiffness values). The points on the black diagonal line indicate that the target stiffness value and the stiffness estimate coincide; (a) small-sized dummy finger, (b) large-sized dummy finger.

TABLE IV
ESTIMATION OF HIGH STIFFNESS USING THE ML-BASED MODELS (MEAN AND STANDART DEVIATION OF NINE ESTIMATES)

Model		Estimated Stiffness Values (Nmm/deg)		
		DIP	***PIP***	***MCP***
MLP	k_{spring}	3.96 ± 0.21	**4.04 ± 0.09**	3.45 ± 0.08
	Δk	3.64 ± 0.39	7.47 ± 0.40	8.60 ± 0.44
CNN	k_{spring}	3.29 ± 0.12	3.54 ± 0.08	2.36 ± 0.04
	Δk	2.06 ± 0.09	7.34 ± 0.46	**7.53 ± 0.39**
LR	k_{spring}	3.59 ± 0.15	3.71 ± 0.12	3.02 ± 0.10
	Δk	**5.16 ± 0.69**	8.40 ± 0.48	9.22 ± 0.42
SVR	k_{spring}	1.40 ± 0.36	1.29 ± 0.00	0.94 ± 0.00
	Δk	5.71 ± 1.47	8.09 ± 0.49	9.89 ± 0.47

Bold numbers indicate the best model for estimating high stiffness values.

themselves resulting from the variation of the finger length. Usually, the finger length changes as it flexes and extends, but the bottom of the Modular-SECA does not expand or contract. In addition, the connectors that connect the Modular-SECAs are designed to match the length of each finger joint when it is flat (i.e., at 0°) [13]. Therefore, as the finger's bending angle increases, the Modular-SECA exerts force in the direction of finger extension in an attempt to prevent a change in the finger length. In our previous study [15], this effect was not as apparent because only the MCP joint was driven to measure its stiffness. However, in this study, the stiffness values of all three joints were measured; thus, the length changes caused by each joint's movement may have affected the interactions between the Modular-SECAs themselves. In particular, the $k_{0.7analytic}$ of the PIP joint was estimated to be considerably smaller than k_{spring} owing to the influence of the two Modular-SECAs of the DIP and MCP.

A comparison of the $k_{0.7analytic}$ results shown in Figs. 2 and 3 reveals that $k_{0.7analytic}$ is significantly different for various finger sizes. One major reason is that when accommodating the Modular-SECAs to fingers of different sizes, connectors with suitably varied lengths need to be used, which causes different interactions between the Modular-SECAs and the finger, even if the same Velcro are used to fix the Modular-SECAs to the

TABLE V
MEAN AND MEAN ABSOLUTE DEVIATION OF THE RMSPE AND MAPD FOR THE PREDICTION DATASETS

Model		DIP		PIP		MCP	
		$RMSPE_{all}$ (%)	$MAPD_{all}$ (%)	$RMSPE_{all}$ (%)	$MAPD_{all}$ (%)	$RMSPE_{all}$ (%)	$MAPD_{all}$ (%)
$k_{0.7analytic}$		201 ± 48	114 ± 80	342 ± 96	46 ± 29	91 ± 32	27 ± 7
MLP	k_{spring}	44 ± 22	9 ± 2	53 ± 28	7 ± 3	53 ± 19	8 ± 4
	Δk	86 ± 36	27 ± 22	98 ± 59	12 ± 6	62 ± 29	17 ± 8
CNN	k_{spring}	40 ± 16	10 ± 5	33 ± 6	5 ± 2	64 ± 34	8 ± 5
	Δk	70 ± 31	16 ± 9	105 ± 78	13 ± 7	96 ± 91	40 ± 28
LR	k_{spring}	105 ± 34	40 ± 25	112 ± 68	35 ± 31	213 ± 175	17 ± 11
	Δk	209 ± 112	111 ± 90	157 ± 105	91 ± 60	151 ± 48	23 ± 14
SVR	k_{spring}	71 ± 18	20 ± 3	58 ± 15	8 ± 5	162 ± 109	6 ± 5
	Δk	89 ± 53	24 ± 5	104 ± 85	59 ± 62	77 ± 51	12 ± 5

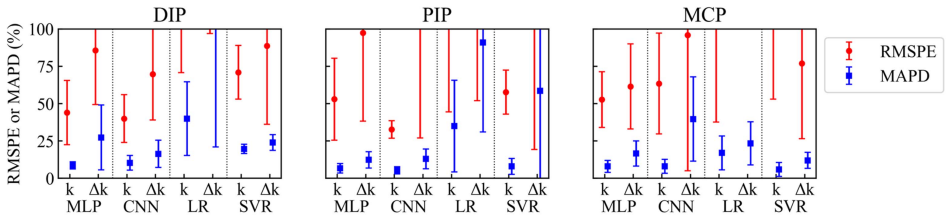

Fig. 4. $RMSPE_{all}$ and $MAPD_{all}$ for the ML-based models of the prediction datasets. k_{spring} is simplified as k. Note that the scale ranges from 0 to 100%.

finger. The $k_{0.7analytic}$ differed depending on the finger size due to changes in the interaction between the finger and the Modular-SECAs. Furthermore, the $k_{0.7analytic}$ variation (standard deviation) is considerable because the interaction between the Modular-SECAs and the finger varies from measurement to measurement. Thus, when estimating joint stiffness values using the Modular-SECAs, the interaction between the Modular-SECAs and the finger must be considered. The ML-based models are likely to "absorb" the effects of these interactions better than the adapted analytical model.

Comparing the results of the ML-based models with different output variables, both the $RMSPE_{all}$ and $MAPD_{all}$ indicate that the models for predicting k_{spring} demonstrate better accuracy than the models for predicting Δk, except for the LR and the SVR for the MCP (Table V). However, in Table III, particularly for the MCP in the M-Test and the S-Prediction, the models for predicting Δk show better the RMSPE in most cases. This is because of the higher accuracy of the adapted analytical model. As shown in Figs. 2 and 3, the models for predicting Δk show similarities in estimation trends with $k_{0.7analytic}$. Hence, the information of the adapted analytical model can guide the training process for predicting Δk. As the MCP joints in the M-Test and the S-Prediction originally have better accuracy than the DIP and PIP in terms of $k_{0.7analytic}$, the accuracy of models for predicting Δk are likely better. However, due to the influence of $k_{0.7analytic}$ accuracy, the $RMSPE_{all}$ exhibit significant variance (Table V and Fig. 4). Therefore, the output variable, k_{spring}, is more suitable for stable and accurate stiffness estimation.

When output variables are the same, the LR tends to have more significant the $MAPD_{all}$ than other algorithms, except for when predicting Δk in the MCP. This suggests that the LR may not effectively absorb the impact of inter-measurement variability, indicating linear regression algorithms' unsuitability for stiffness estimation. The SVR demonstrates better accuracy than the ANNs in some predictions, such as for the PIP in the M-Test. However, especially in the MCP joints, the $RMSPE_{all}$ are poorer than the ANNs, indicating insufficient stability in accuracy. Consequently, compared to other nonlinear regression algorithms, the ANN is suggested as a suitable ML algorithm for stiffness estimation with the Modular-SECA, which involves complex and nonlinear influencing factors.

Therefore, the models for predicting k_{spring} using the MLP or the CNN are the best. However, for the MCP joints, the CNN's $RMSPE_{all}$ is poorer than the other two joints, and the mean is around 60%. While the MLP for the DIP and PIP exhibit worse the $RMSPE_{all}$ than the CNN, they fare better than the CNN of the MCP. Hence, the MLP consistently achieves better accuracy across all joints. The small size of the training data in this study may have caused the model to overfit the training data due to the deeper features extracted by the convolutional layers of the CNN, resulting in lower generality than the MLP. The characteristics of the CNN could become more effective with more training data. Thus, we determined that among the ML-based models proposed in this study, the best model for stiffness estimation was the model for predicting k_{spring} using the MLP.

In this study, the simultaneous estimation of the stiffness values of the DIP, PIP, and MCP joints using joint modular soft actuators was performed by incorporating the ANN models. To the best of our knowledge, this is the first time an ANN model has been proposed for stiffness estimation using joint modular soft actuators. The generality and repeatability of the proposed ANN models for different finger sizes and higher stiffness values were also tested and further compared with other ML algorithms.

However, this study has some limitations.

- Proving the validity of the stiffness estimation of human finger joints using the ANN models is challenging. Comparisons with other assessment methods, such as ground-truth measurements, as in [17], or clinical measures with the help of clinicians, are necessary.

- The joint angle-air pressure relationship is a dynamic process that is affected by the inflow rate of air pressure [25]. Therefore, an appropriate inflow velocity that stabilizes the joint angle and, thus, the stiffness estimation accuracy, should be considered.
- In the stiffness estimation, the joint angle must be within the range of $0 \leq \theta < \theta_0$. However, in some cases, the joint angle may be θ_0 before the air pressure input to the Modular-SECA reaches 80 kPa. In such cases, the ANN models cannot estimate joint stiffness because the proposed ANN models utilize a pressure-angular change profile up to 80 kPa. Thus, this limitation must be compensated, for example, by predicting the trajectory up to 80 kPa from the obtained angle trajectory.
- The ANN model is likely to be specified only for index fingers due to it being trained with data collected from dummy fingers designed based on the sizes of index fingers. However, the results of the prediction performance of the ANN model for the S-Prediction and the L-Prediction showed that the ANN model could be applied to different finger sizes. Therefore, the ANN model for the index finger may predict joint stiffness for other fingers; thus, we should validate with dummy other fingers.

V. Conclusion

In this study, ANN-based models are proposed to simultaneously estimate the stiffness of the DIP, PIP, and MCP joints. By utilizing the ANNs, we can model the effects of the complex behaviors due to the interactions between the finger and the Modular-SECAs and due to the interaction between the Modular-SECAs themselves, which cannot be addressed by employing the adapted analytical model. Unlike the adapted analytical model, which averages the estimated stiffness of the individual points of each pressure-angular change profile, the ANN models fully utilize the pressure-angular change profile. Consequently, the stiffness of finger joints can be estimated more stably, accurately, and quantitatively than by using the adapted analytical model. Additionally, the results show that the ANNs may be superior to other ML algorithms as a stiffness estimation model in terms of generality and repeatability. In the future, we need to consider how to determine the reliability of predictions using the ANN models.

References

[1] V. Dietz and T. Sinkjaer, "Spastic movement disorder: Impaired reflex function and altered muscle mechanics," *Lancet Neurol.*, vol. 6, no. 8, pp. 725–733, 2007, doi: 10.1016/S1474-4422(07)70193-X.

[2] G. P. Sadarangani, X. Jiang, L. A. Simpson, J. J. Eng, and C. Menon, "Force myography for monitoring grasping in individuals with stroke with mild to moderate upper-extremity impairments: A preliminary investigation in a controlled environment," *Front. Bioeng. Biotechnol.*, vol. 5, Jul. 2017, Art. no. 42, doi: 10.3389/fbioe.2017.00042.

[3] J. Plantin et al., "Quantitative assessment of hand spasticity after stroke: Imaging correlates and impact on motor recovery," *Front. Neurol.*, vol. 10, Aug. 2019, Art. no. 836, doi: 10.3389/fneur.2019.00836.

[4] R. W. Bohannon and M. B. Smith, "Interrater reliability of a modified Ashworth scale of muscle spasticity," *Phys. Ther.*, vol. 67, no. 2, pp. 206–207, Feb. 1987, doi: 10.1093/ptj/67.2.206.

[5] J.-H. Park et al., "Development of elbow spasticity model for objective training of spasticity assessment of patients post stroke," in *Proc. Int. Conf. Rehabil. Robot.*, 2017, pp. 146–151, doi: 10.1109/ICORR.2017.8009237.

[6] J. F. M. Fleuren et al., "Stop using the Ashworth scale for the assessment of spasticity," *J. Neurol., Neurosurgery, Psychiatry*, vol. 81, no. 1, pp. 46–52, Jan. 2010, doi: 10.1136/jnnp.2009.177071.

[7] Y. Tomita et al., "Development of a stiffness measurement system and biomechanical model of ankle joint to evaluate viscoelasticity and muscle contraction," *Japanese J. Comprehensive Rehabil. Sci.*, vol. 5, pp. 147–155, 2014, doi: 10.11336/jjcrs.5.147.

[8] D. G. Kamper and W. Z. Rymer, "Quantitative features of the stretch response of extrinsic finger muscles in hemiparetic stroke," *Muscle Nerve*, vol. 23, no. 6, pp. 954–961, Jun. 2000, doi: 10.1002/(sici)1097-4598(200006)23:6<954::aid-mus17>3.0.co;2-0.

[9] E. Peperoni et al., "Self-aligning finger exoskeleton for the mobilization of the metacarpophalangeal joint," *IEEE Trans. Neural Syst. Rehabil. Eng.*, vol. 31, pp. 884–894, 2023, doi: 10.1109/TNSRE.2023.3236070.

[10] R. Ranzani, G. Chiriatti, A. Schwarz, G. Devittori, R. Gassert, and O. Lambercy, "An online method to monitor hand muscle tone during robot-assisted rehabilitation," *Front. Robot. AI*, vol. 10, Feb. 2023, Art. no. 1093124, doi: 10.3389/frobt.2023.1093124.

[11] H. L. Heung, Z. Q. Tang, X. Q. Shi, K. Y. Tong, and Z. Li, "Soft rehabilitation actuator with integrated post-stroke finger spasticity evaluation," *Front. Bioeng. Biotechnol.*, vol. 8, Feb. 2020, Art. no. 111, doi: 10.3389/fbioe.2020.00111.

[12] S.-S. Yun, B. B. Kang, and K.-J. Cho, "Exo-glove PM: An easily customizable modularized pneumatic assistive glove," *IEEE Robot. Autom. Lett.*, vol. 2, no. 3, pp. 1725–1732, Jul. 2017, doi: 10.1109/LRA.2017.2678545.

[13] S. Kokubu et al., "Evaluation of fiber-reinforced modular soft actuators for individualized soft rehabilitation gloves," *Actuators*, vol. 11, no. 3, Mar. 2022, Art. no. 84, doi: 10.3390/act11030084.

[14] S. Kokubu, P. E. T. Vinocour, and W. Yu, "Development and evaluation of fiber reinforced modular soft actuators and an individualized soft rehabilitation glove," *Robot. Auton. Syst.*, vol. 171, Jan. 2024, Art. no. 104571, doi: 10.1016/j.robot.2023.104571.

[15] F. Matsunaga et al., "Finger joint stiffness estimation with joint modular soft actuators for hand telerehabilitation," *Robotics*, vol. 12, no. 3, Jun. 2023, Art. no. 83, doi: 10.3390/robotics12030083.

[16] C. Q. Zhou, X. Q. Shi, Z. Li, and K. Y. Tong, "3D printed soft robotic hand combining post-stroke rehabilitation and stiffness evaluation," in *Proc. 15th Int. Conf. Intell. Robot. Appl.*, 2022, pp. 13–23, doi: 10.1007/978-3-031-13835-5_2.

[17] X. Q. Shi, H. L. Heung, Z. Q. Tang, K. Y. Tong, and Z. Li, "Verification of finger joint stiffness estimation method with soft robotic actuator," *Front. Bioeng. Biotechnol.*, vol. 8, Dec. 2020, Art. no. 592637, doi: 10.3389/fbioe.2020.592637.

[18] G. L. Goh et al., "Joint angle prediction for a cable-driven gripper with variable joint stiffness through numerical modeling and machine learning," *Int. J. AI Mater. Des.*, vol. 1, no. 1, Jan. 2024, Art. no. 62, doi: 10.36922/ijamd.2328.

[19] N. Sengupta, A. S. Rao, B. Yan, and M. Palaniswami, "A survey of wearable sensors and machine learning algorithms for automated stroke rehabilitation," *IEEE Access*, vol. 12, pp. 36026–36054, 2024, doi: 10.1109/ACCESS.2024.3373910.

[20] E. Halilaj, A. Rajagopal, M. Fiterau, J. L. Hicks, T. J. Hastie, and S. L. Delp, "Machine learning in human movement biomechanics: Best practices, common pitfalls, and new opportunities," *J. Biomech.*, vol. 81, pp. 1–11, Nov. 2018, doi: 10.1016/j.jbiomech.2018.09.009.

[21] Y. J. Choo and M. C. Chang, "Use of machine learning in stroke rehabilitation: A narrative review," *Brain Neurorehabilitation*, vol. 15, no. 3, 2022, Art. no. e26, doi: 10.12786/bn.2022.15.e26.

[22] 2024. [Online]. Available: https://github.com/Fuko-Matsunaga/joint-stiffness-estimation-experiment-using-dummy-fingers

[23] M. Kuhn and K. Johnson, *Applied Predictive Modeling*. Berlin, Germany: Springer, 2013.

[24] W. Dai, J. Y. Wu, and C. J. Lu, "Combining nonlinear independent component analysis and neural network for the prediction of Asian stock market indexes," *Expert Syst. Appl.*, vol. 39, no. 4, pp. 4444–4452, Mar. 2012, doi: 10.1016/j.eswa.2011.09.145.

[25] D. G. Kamper, H. C. Fischer, E. G. Cruz, and W. Z. Rymer, "Weakness is the primary contributor to finger impairment in chronic stroke," *Arch. Phys. Med. Rehabil.*, vol. 87, no. 9, pp. 1262–1269, Sep. 2006, doi: 10.1016/j.apmr.2006.05.013.